Electronic Supplementary Information

Gradient-Temperature Hydrothermal Fabrication of Hierarchical Zn_2SnO_4 Hollow Boxes Stimulated by Thermodynamic Phase Transformation

Xiong Liu,‡ Chaojiang Niu,‡ Jiashen Meng,‡ Xiaoming Xu, Xuanpeng Wang, Bo Wen, Ruiting Guo and Liqiang Mai*

State Key Laboratory of Advanced Technology for Materials Synthesis and Processing, Wuhan University of Technology, Wuhan 430070, P. R. China. E-mail: mlq518@whut.edu.cn.

‡ These authors contributed equally to this work.

* Corresponding authors: mlq518@whut.edu.cn

Experimental Section

Preparation of hierarchical Zn_2SnO_4 hollow boxes: Firstly, 0.3 mmol $SnCl_4{\cdot}5H_2O$ (AR), 0.3 mmol $C_4H_6O_4Zn{\cdot}2H_2O$ (AR), 3 mmol NaOH (AR) were dissolved in 40 mL deionized water. After the raw materials were completely dissolved at room temperature (~5 min), the muddy precursor solution was transferred into 50 mL sealed Teflon autoclave. And the reaction was carried out at 130 °C for 6 h then at 200 °C for 26 h in the homothermal oven. Noting that all the precursors seal in sealed Teflon autoclave without disturbances during whole continuous low and high temperature processing. Finally, the products were obtained after washing with ethanol and drying in vacuum at 70 °C for 12 h. Meanwhile, Zn_2SnO_4 nanosheets were obtained without reaction at 130 °C. And the $ZnSnO_3$ solid microcubes were obtained without reaction at 200 °C.

Preparation of Zn_2SnO_4 hollow microspheres: 0.5 g sodium stannate tetrahydrate ($Na_2SnO_3{\cdot}4H_2O$, AR), 35 mg sodium alginate ($(C_6H_7NaO_6)_n$, CP), 0.7665 g $C_4H_6O_4Zn{\cdot}2H_2O$ (AR) and 8 mL $NH_3{\cdot}H_2O$ were dissolved in 32 mL deionized water. After the raw materials were completely dissolved at room temperature (about 5 min), the milky precursor solution was transferred into 50 mL sealed Teflon autoclave. And the reaction was carried out at 160 °C for 6 h then at 180 °C for 12 h in the homothermal oven, respectively. Finally, the products were obtained after washing with ethanol and

drying in vacuum at 70 °C for 12 h. Meanwhile, the $ZnSnO_3$ solid microspheres were obtained without reaction at 180 °C.

Preparation of Zn_2SnO_4 hollow nanoboxes: Firstly, 0.3 mmol $SnCl_4 \cdot 5H_2O$ (AR), 0.3 mmol $C_4H_6O_4Zn \cdot 2H_2O$ (AR), 3 mmol NaOH (AR) were dissolved in 40 mL deionized water. The raw materials were completely dissolved and reacting at 60 °C for 6 h in water bath. Then the reaction was carried out 200 °C for 12 h in the homothermal oven. Finally, the products were obtained after washing with ethanol and drying in vacuum at 70 °C for 12 h. The $ZnSn(OH)_6$ solid nanocubes were obtained without reaction at 200 °C.

Preparation of Co-ZIF hollow polyhedron: First, under the condition of room-temperature stir, the methanol solution with 1.5000 g $Co(NO_3)_2 \cdot 6H_2O$ were dropped into the methanol solution with 0.5000 g 2-Methylimidazole slowly and evenly. After stirring for 6 h, the whole solution was sealed in 50 mL sealed Teflon autoclave. And the reaction was carried out at 120 °C for 24 h in the homothermal oven. Finally, the products were obtained after washing with ethanol and drying in vacuum at 70 °C for 12 h. The Co-ZIF-67 solid polyhedron was obtained without reaction at 120 °C.

Morphology and structure characterization: The crystallographic information of the final products was measured using a Bruker D8 Discover X-ray diffractometer equipped with a Cu Kα radiation source; the samples were scanned over the 2θ range from 3° to 80° at room temperature. SEM images were collected using a JEOL-7100F scanning electron microscope, and TEM images were collected using a JEM-2100F transmission electron microscope. The BET surface area was calculated from nitrogen adsorption isotherms measured at 77 K using a Tristar-3020 instrument.

Concurrent elemental semi-quantitative analysis: These tests are designed to quantify the content of $ZnSnO_3$ and Zn_2SnO_4 phase with the INCA Energy System. As known that SmartMap performs the simultaneous acquisition of X-ray data for all possible elements from each pixel on a user defined area of an image, so we collect X-ray data from the entire area shown in the image using the full field tool. And the semi-quantitative results will be obtained with the atomic content (%) of Zn, Sn and O

elements. Therefore, we can calculate the content of $ZnSnO_3$ and Zn_2SnO_4 phase on the basis of fixed proportion of Zn and Sn in $ZnSnO_3$ and Zn_2SnO_4 phase.

Lithium-ion batteries electrochemical measurements: The 2016 coin cells were assembled in a glovebox filled with pure argon gas. Lithium foil was used as the anode and a solution of $LiPF_6$ (1 M) in EC/DEC (1:1 vol/vol) was used as the electrolyte. The cathode was composed of a ground mixture of active material, acetylene black and poly(tetrafluoroethylene) (PTFE, 90 wt%) as binders, with mass ratio of 6:3:1. After coating onto copper foil, the electrode film was uniformly cut into ~0.5 cm^2 (area) round slices, weighing a total of about 1.0 mg. The corresponding areal mass loading was about 2.0 mg cm^{-2}. Galvanostatic charge/discharge measurements were performed using a multichannel battery testing system (LAND CT2001A). Cyclic voltammograms and electrochemical impedance spectra werek collected at room temperature using an Autolabpotentiostat/galvanostat. In addition, the calculated capacity was based on the mass of active materials.

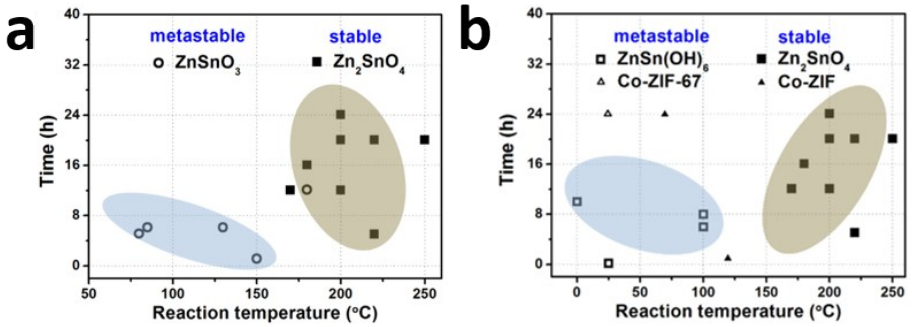

Fig. S1 A large number of literatures survey results in the forms of data, which represents the synthesis temperature and reaction time of materials.

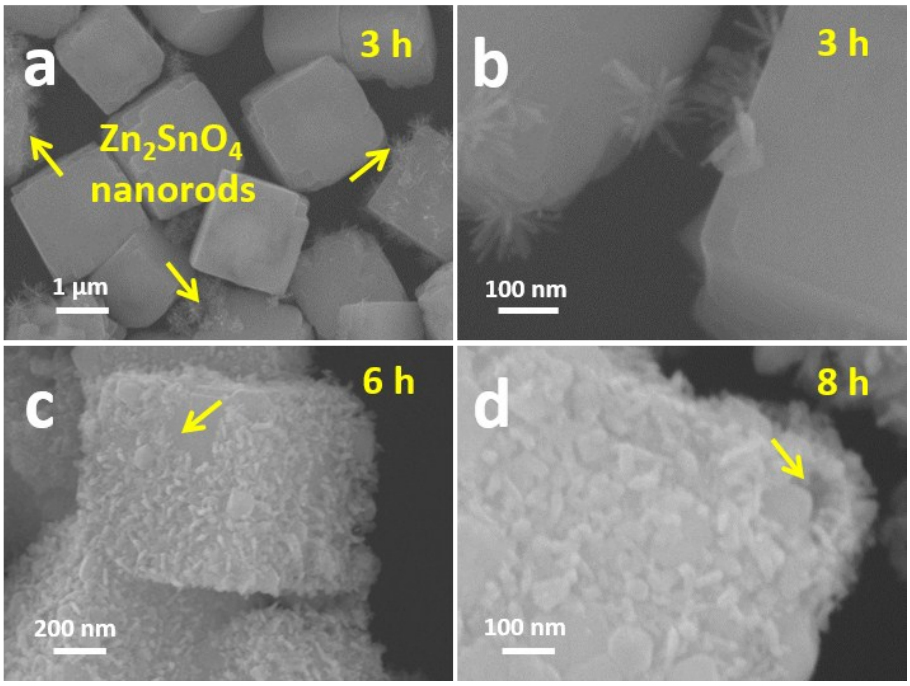

Fig. S2 SEM images of samples prepared at 200 °C for 3 h (a-b), 6 h (c) and 8 h (d). Noting that all samples have gone through hydrothermal treatment at 130 °C for 6 h before reacting at 200 °C.

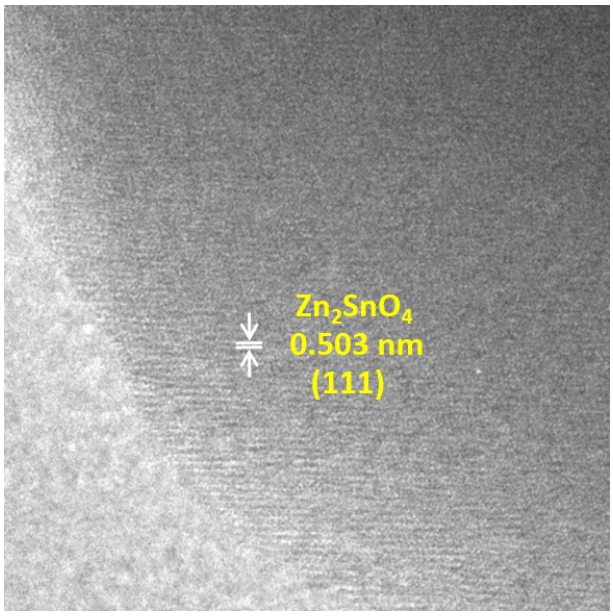

Fig. S3 High resolution TEM of external shell of $ZnSnO_3$@Zn_2SnO_4 yolk-shelled microcube in Fig. 2a.

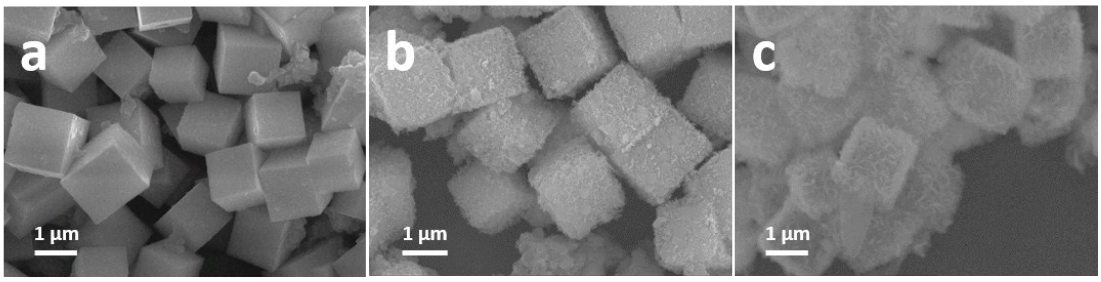

Fig. S4 SEM images of $ZnSnO_3$ microcubes (a), $ZnSnO_3$ @Zn_2SnO_4 yolk-shelled microcubes (b) and Zn_2SnO_4 hollow boxes (c).

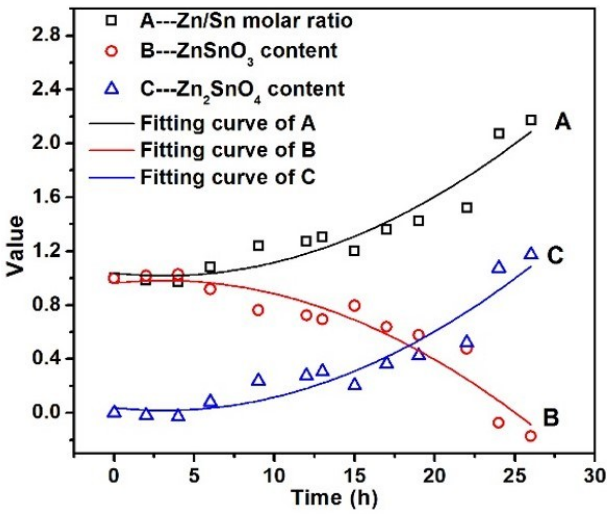

Fig. S5 Semi-quantitative results with EDS analysis.

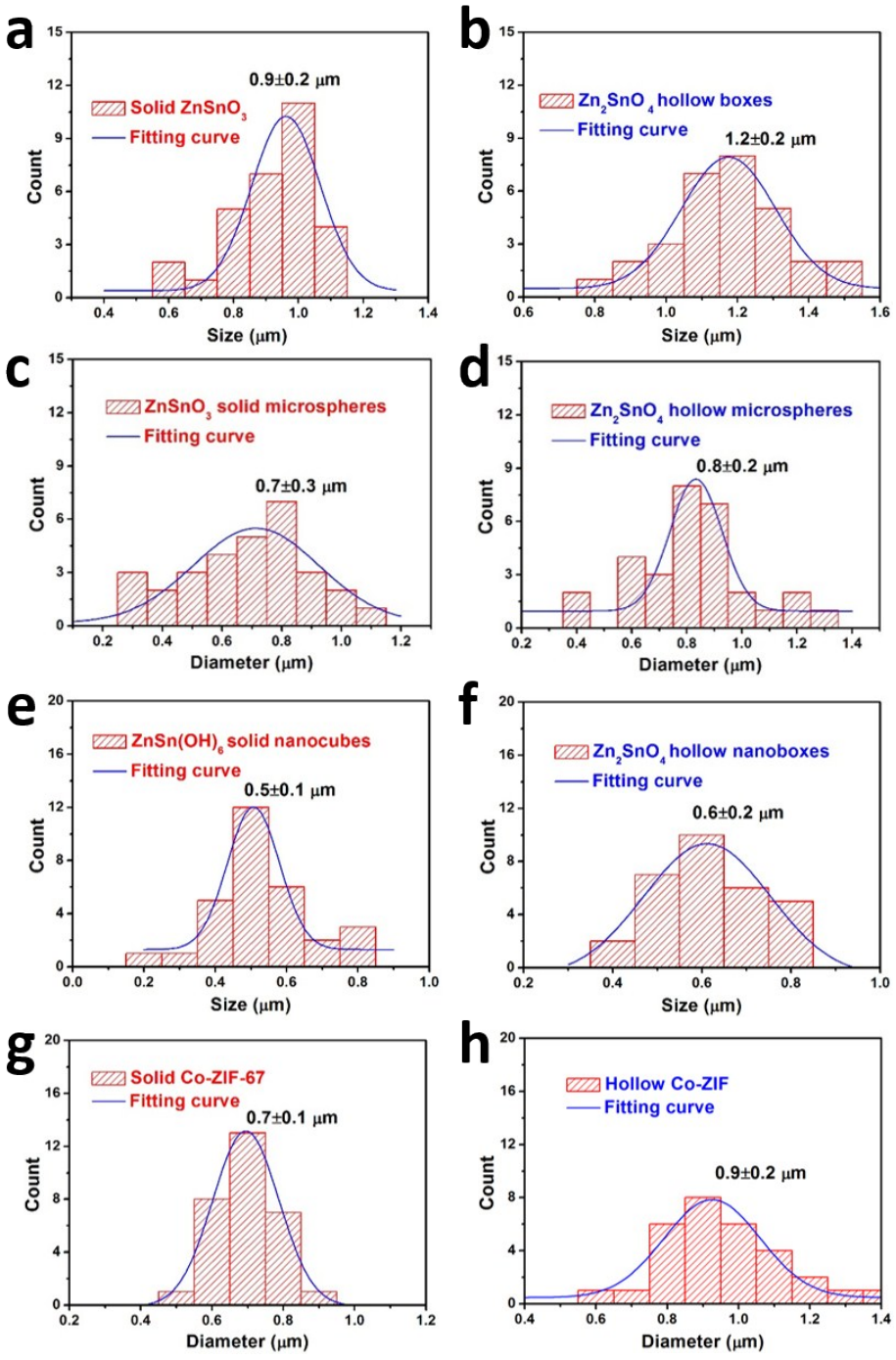

Fig. S6 Geometrical characteristics of $ZnSnO_3$ solid microcubes (a) and Zn_2SnO_4 hollow boxes (b); $ZnSnO_3$ solid microspheres (c), Zn_2SnO_4 hollow microspheres (d), $ZnSn(OH)_6$ solid nanocubes (e), Zn_2SnO_4 hollow nanoboxes (f); solid Co-ZIF-67 (g) and hollow Co-ZIF (h) in a large selected SEM area via size statistics methods.

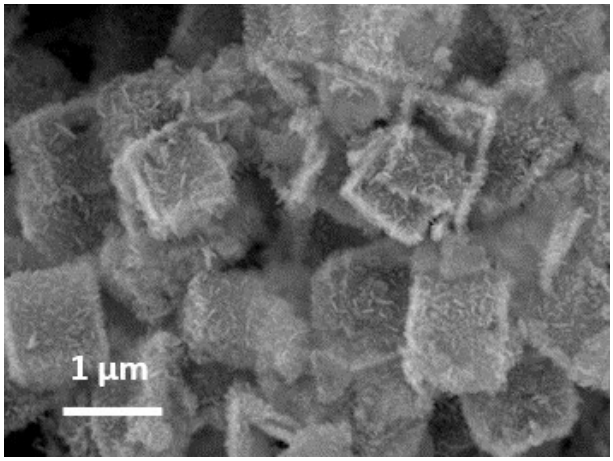

Fig. S7 SEM image of Zn_2SnO_4 hollow boxes prepared at 200 °C for 36 h.

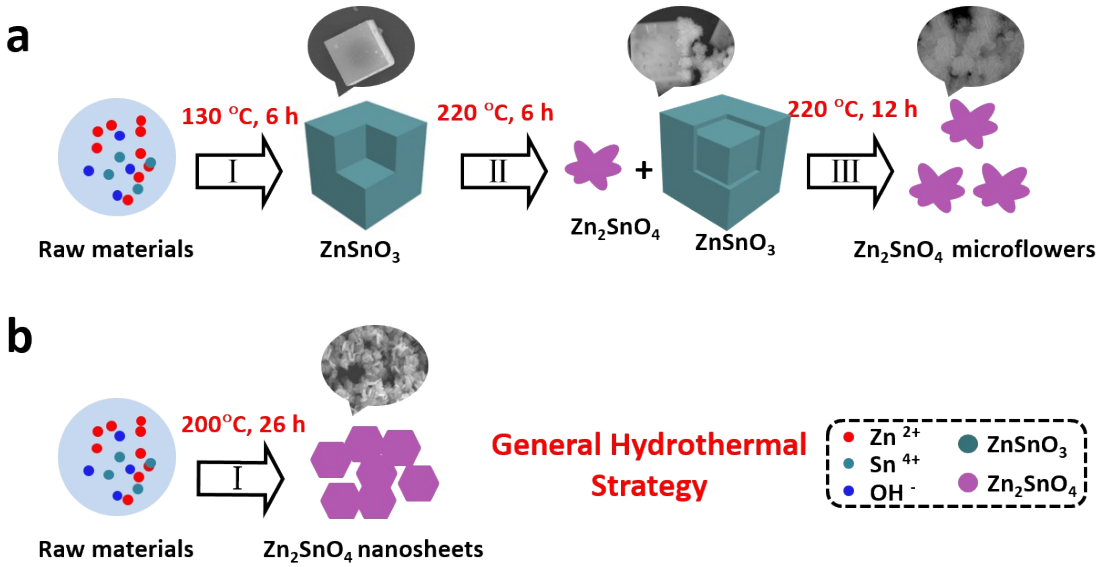

Scheme S1 a) Schematic illustrations of synthesis processing of Zn_2SnO_4 microflowers with morphology evolution under a gradient-temperature hydrothermal strategy. b) Schematic illustrations of synthesis processing of Zn_2SnO_4 nanosheets under a general hydrothermal strategy.

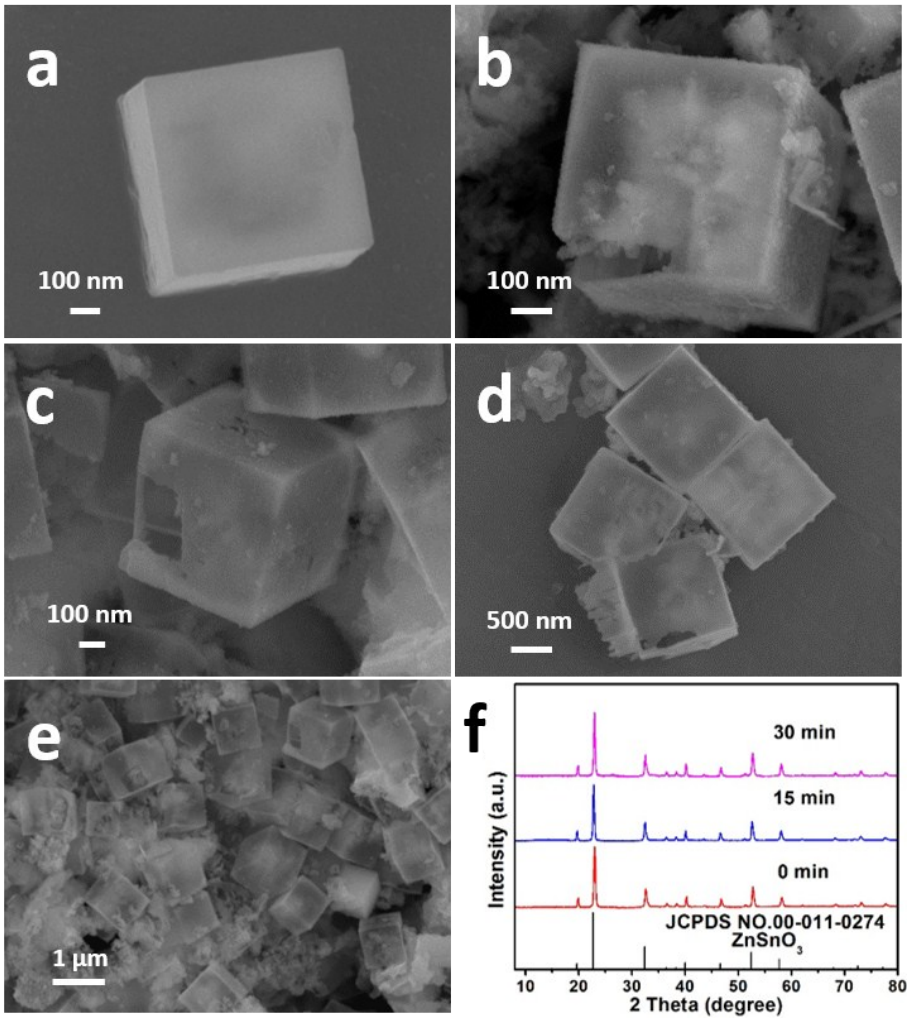

Fig. S8 The detailed process of the formation of hollow $ZnSnO_3$ microcubes via alkaline corrosion method. The whole preparation processes are as follows: First of all, 40 mg of the obtained $ZnSnO_3$ microcubes were dispersed in 0.5 M NaOH aqueous solution, then stirred for several time at room temperature, finally centrifuged and dried the products. It is evident that the sequential structural transformation from solid to yolk-shelled and then hollow structure could be exhibited in SEM images of (a), (b), (c-e), with reaction of 0, 15, 30 min, respectively.

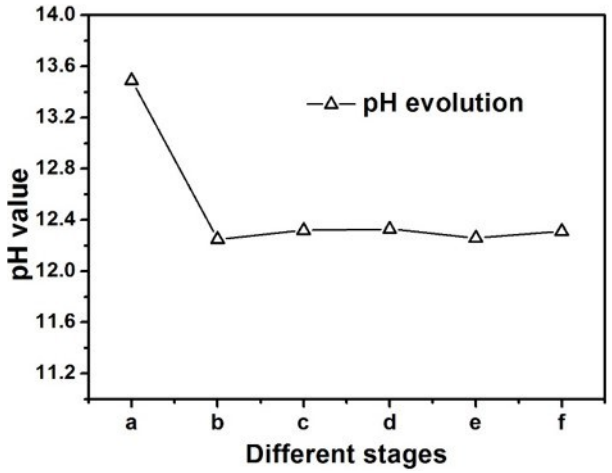

Fig. S9 The pH values of supernatant solution at different stages during gradient-temperature hydrothermal process, measured by pH detector. (a) precursor solution before hydrothermal process; (b) after 130 °C for 6 h; (c-f) after 130 °C for 6 h, then with reaction time of 1 h (c), 5 h (d), 12 h (e) and 26 h (f) at 200 °C.

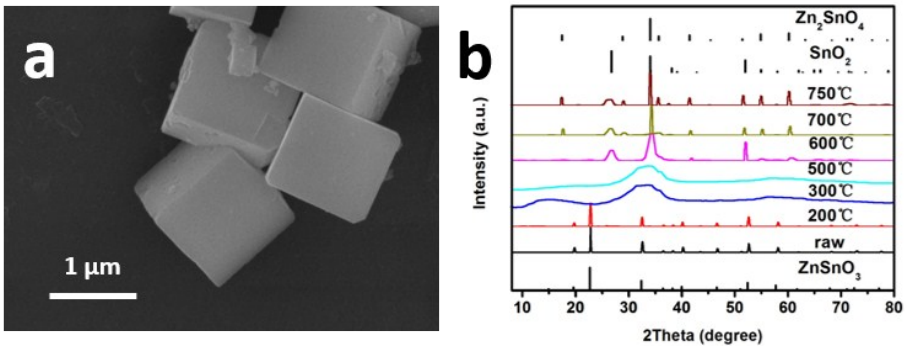

Fig. S10 The calcination process of $ZnSnO_3$ microcubes. (a) SEM image of $ZnSnO_3$ microcubes after sintering at 200 °C in air for 6 h. (b) The typical XRD pattern showing the phase change with different calcination temperature in air for 6 h.

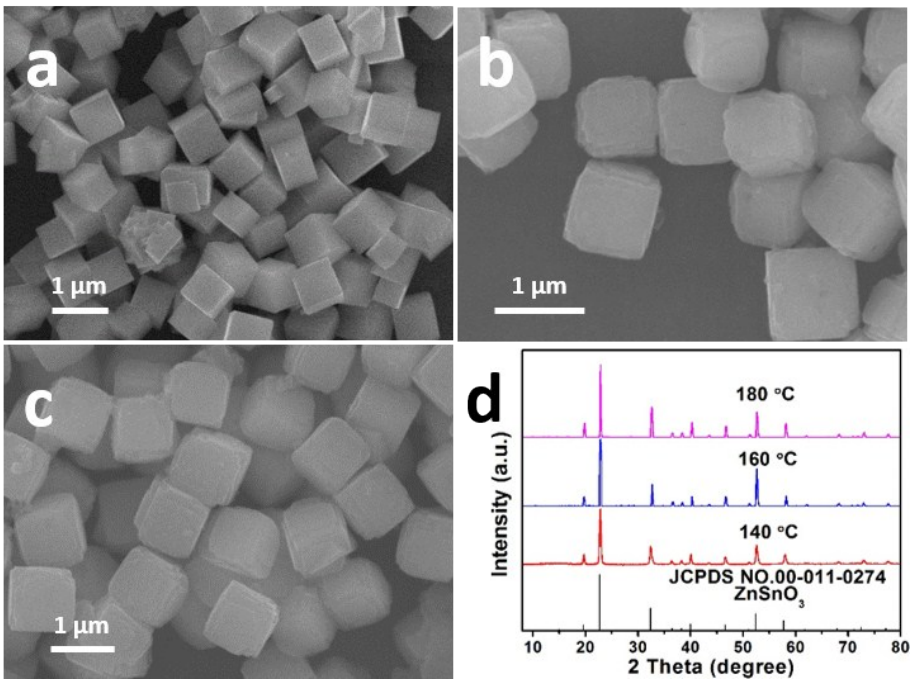

Fig. S11 SEM images of products prepared at 140 °C (a), 160 °C (b), 180 °C (c) for 24 h, respectively. d) The corresponding XRD pattern.

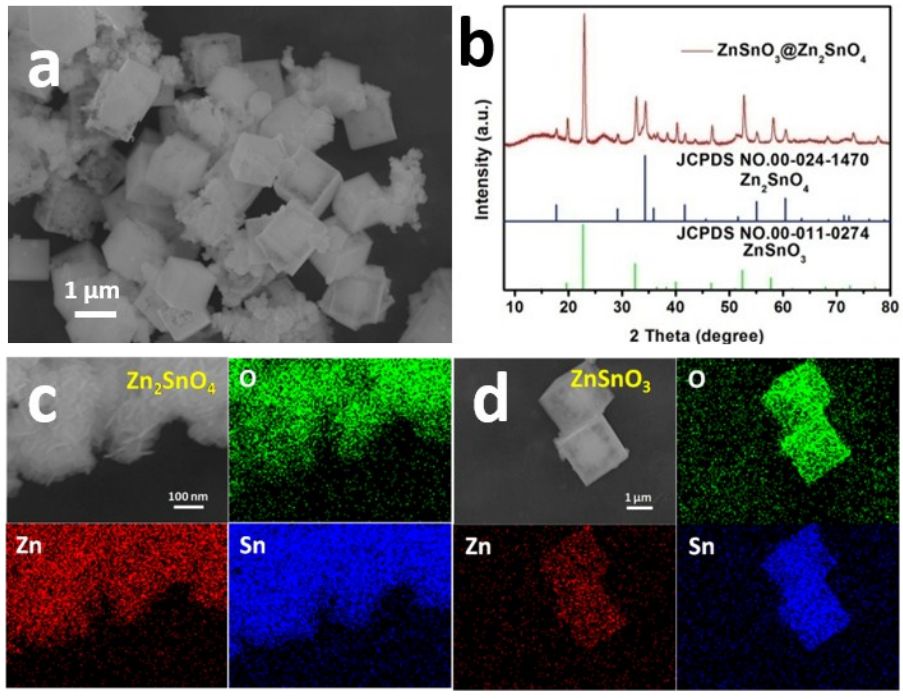

Fig. S12 SEM images (a) and XRD patterns (b) of mixed yolk-shelled $ZnSnO_3$ and aggregative Zn_2SnO_4 microflowers products. EDS elemental mappings of aggregative Zn_2SnO_4 microflowers (c) and yolk-shelled $ZnSnO_3$ (d), which were selected from (a).

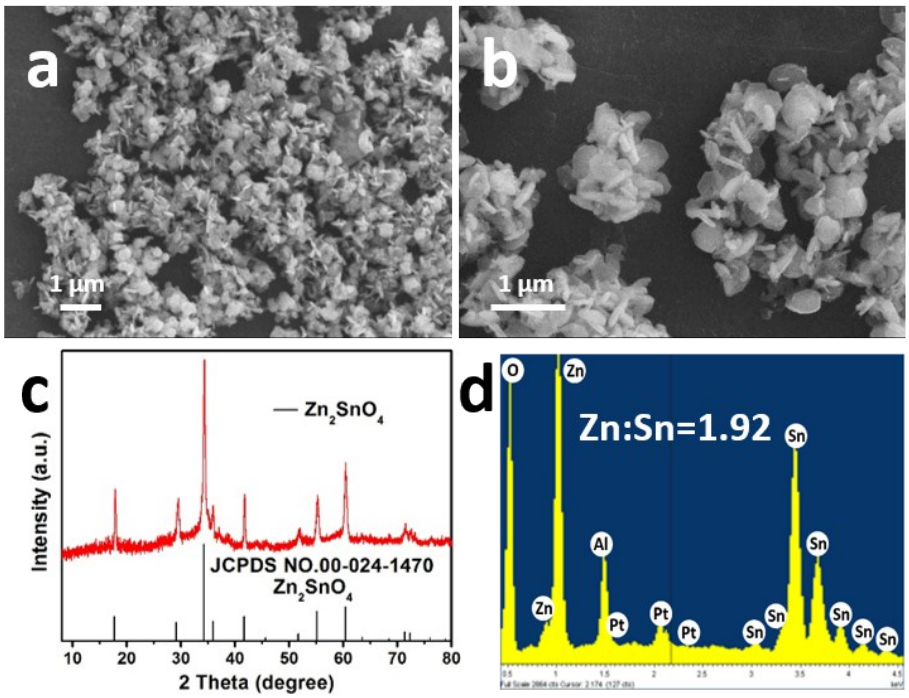

Fig. S13 SEM images (a, b), XRD pattern (c) and EDS spectrum of Zn_2SnO_4 nanosheets.

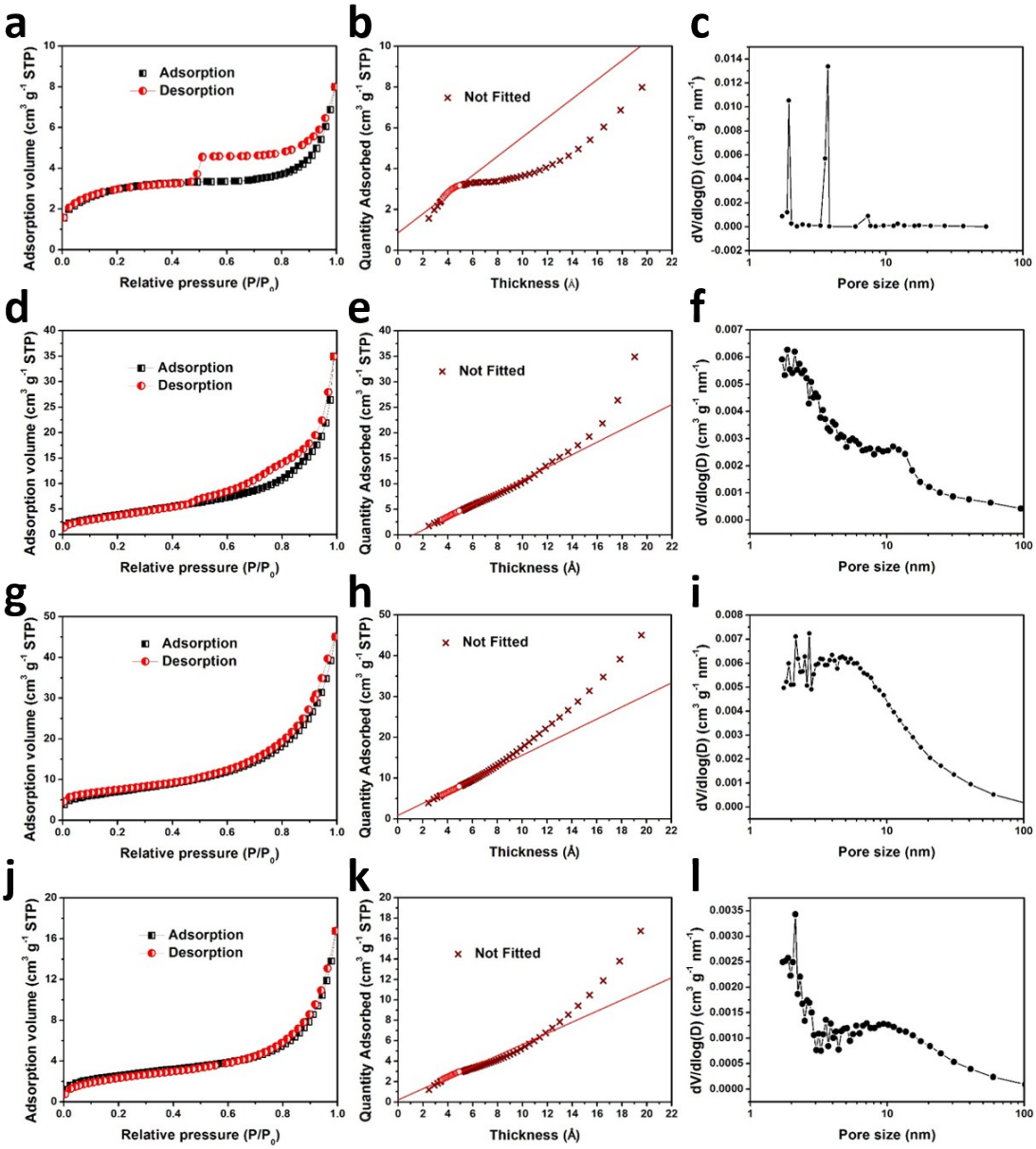

Fig. S14 a-c) Nitrogen absorption/desorption isotherm (a), t-plot curve (b) and BJH pore size distribution (c) of $ZnSnO_3$ solid microcubes. d-f) Nitrogen absorption/desorption isotherm (d), t-plot curve (e) and BJH pore size distribution (f) of $ZnSnO_3$@Zn_2SnO_4 yolk-shelled microcubes. g-i) Nitrogen absorption/desorption isotherm (g), t-plot curve (h) and BJH pore size distribution (i) of Zn_2SnO_4 hollow boxes. j-l) Nitrogen absorption/desorption isotherm (j), t-plot curve (h) and BJH pore size distribution (i) of Zn_2SnO_4 nanosheets.

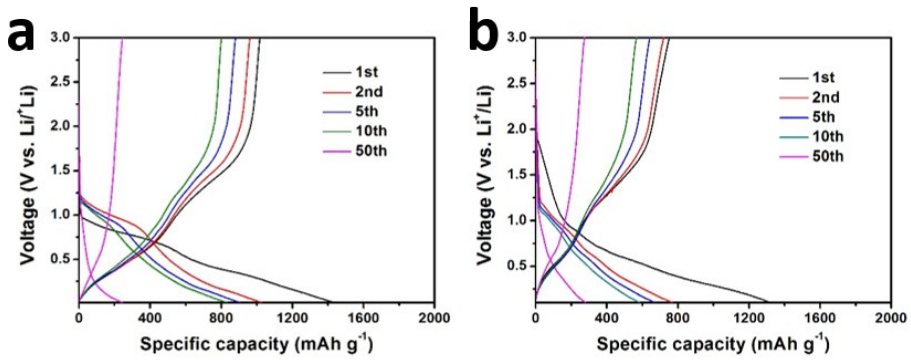

Fig. S15 Charge-discharge curves of Zn_2SnO_4 nanosheets (a) and $ZnSnO_3$ solid microcubes (b) at 200 mA g^{-1} vs. Li^+/Li in the potential of 0.1-3.0 V.

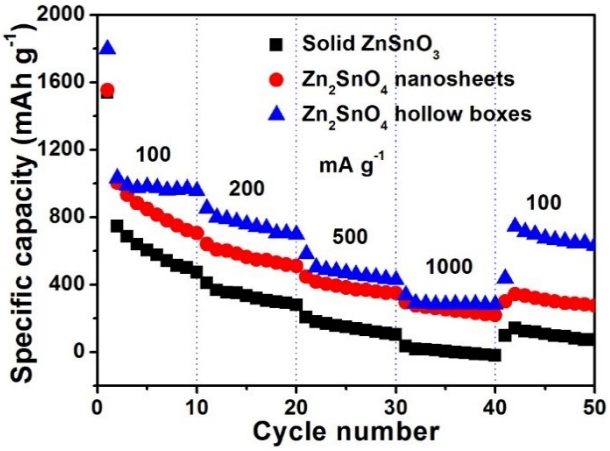

Fig. S16 Rate performances of Zn_2SnO_4 hollow boxes, Zn_2SnO_4 nanosheets and ZnSnO3 solid microcubes.

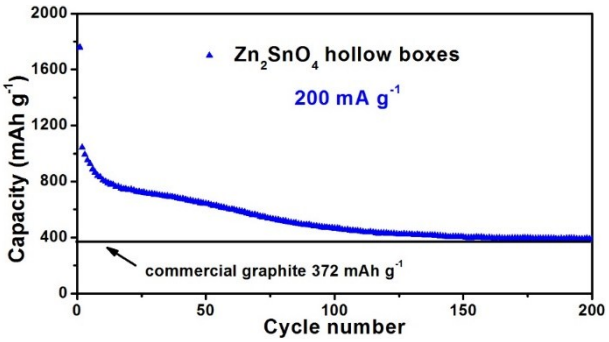

Fig. S17 Long-life cycling performance of Zn_2SnO_4 hollow boxes at 200 mA g^{-1} in the potential of 0.1-3.0 V.

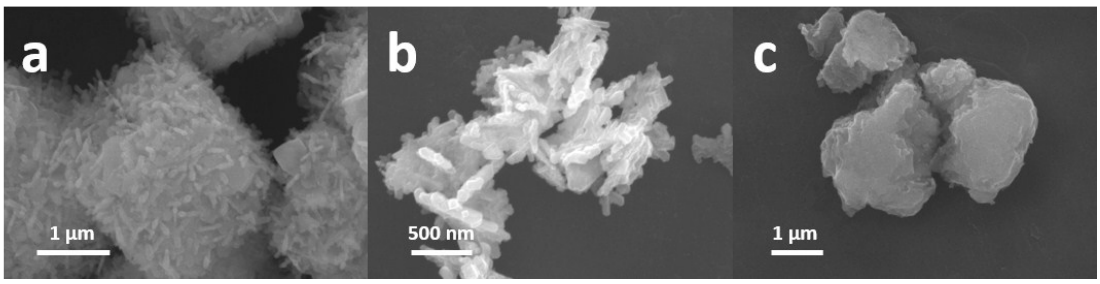

Fig. S18 SEM images of Zn_2SnO_4 hollow boxes (a), Zn_2SnO_4 nanosheets (b) and $ZnSnO_3$ solid microcubes (c) after 30 cycles at 200 mA g^{-1} vs. Li^+/Li in the potential of 0.1-3.0 V.

Table S1. Summary of crystal structure information.[32]

Parameters	**$ZnSnO_3$**	**Zn_2SnO_4**
Reference code	00-011-0274	00-024-1470
Crystal system	Rhombohedral	Cubic
Space group	R3c	Fd-3m
a	5.2600	8.6574
b	5.2600	8.6574
c	14.0000	8.6574
α	-	90.0000
β	-	90.0000
γ	-	90.0000

Table S2. Summary of concurrent elemental semi-quantitative analysis.

Reaction time (h)	Zn atomic (%)	Sn atomic (%)	Zn/Sn molar ratio	$ZnSnO_3$ content	Zn_2SnO_4 content
0	6.6	6.6	1	1	0
2	7.69	7.82	0.98	1.01	-0.01
4	5.28	5.43	0.97	1.02	-0.02
6	6.04	5.58	1.08	0.92	0.08
9	12.15	9.81	1.24	0.76	0.24
12	8.02	6.29	1.28	0.72	0.28
13	12.49	9.56	1.31	0.69	0.31
15	11.08	9.20	1.20	0.80	0.2
17	12.32	9.05	1.37	0.64	0.36
19	13.38	9.40	1.42	0.58	0.42
22	14.30	9.39	1.52	0.48	0.52
24	8.23	3.97	2.07	-0.07	1.07
26	13.56	6.24	2.17	-0.17	1.17

Table S3. Summary of nitrogen absorption/desorption results, $ZnSnO_3$ solid microcubes (A), $ZnSnO_3$@Zn_2SnO_4 yolk-shelled microcubes (B), Zn_2SnO_4 hollow boxes (C) and Zn_2SnO_4 nanosheets (D).

Samples	BET Surface Area ($m^2\ g^{-1}$)	Langmuir Surface Area ($m^2\ g^{-1}$)	Average pore diameter (nm)	t-plot micropore volume ($10^{-4}\ cm^3\ g^{-1}$)
A	10.12	14.55	8.97	13.55
B	14.58	21.69	12.53	-
C	24.78	35.73	11.02	8.73
D	9.11	13.22	13.69	2.87

Table S4. Electrochemical performance contrast with previous reports.

Materials	Voltage (V *vs.* Li^+/Li)	Reversible capacity (mAh g^{-1})	Current density (mA g^{-1})	Reference
Hollow Zn_2SnO_4	**0.1-3.0**	**642/50 cycles** **382/50 cycles**	**200** **1000**	**This work**
ex situ carbon coated Zn_2SnO_4 nanoparticals	0.01-3.0	533/50 cycles	700	21
Sheet-like $ZnSnO_3$	0.01-3.0	625/50 cycles	100	22
Hollow Zn_2SnO_4 boxes@Graphane	0.01-2.0	678/45 cycles	300	23
Zn_2SnO_4 nanoparticals	0.05-3.0	521.4/40 cycles	50	24
Layered Zn_2SnO_4/ Graphane	0.005-3.0	688/50 cycles	200	25
Zn_2SnO_4 nanowires	0.005-3.0	695/60 cycles	120	26
Silver-modified hollow $ZnSnO_3$ boxes	0.005-2.5	464.5/45 cycles	300	27
$ZnSnO_3$ –C hollow microcubes	0.01-3.0	703/50 cycles	100	28